

# Properties of $(\text{Ga}_{1-x}\text{In}_x)_2\text{O}_3$ over the whole $x$ range

M B Maccioni, F Ricci and V Fiorentini

CNR-IOM and Dept. of Physics, University of Cagliari, Cittadella Universitaria,  
09042 Monserrato (CA), Italy

E-mail: [vincenzo.fiorentini@dsf.unica.it](mailto:vincenzo.fiorentini@dsf.unica.it)

**Abstract.** Using density-functional ab initio theoretical techniques, we study  $(\text{Ga}_{1-x}\text{In}_x)_2\text{O}_3$  in both its equilibrium structures (monoclinic  $\beta$  and bixbyite) and over the whole range of composition. We establish that the alloy exhibits a large and temperature-independent miscibility gap. On the low- $x$  side, the favored phase is isostructural with  $\beta\text{-Ga}_2\text{O}_3$ ; on the high- $x$  side, it is isostructural with bixbyite  $\text{In}_2\text{O}_3$ . The miscibility gap opens between approximately 15% and 55% In content for the bixbyite alloy grown epitaxially on  $\text{In}_2\text{O}_3$ , and 15% and 85% In content for the free-standing bixbyite alloy. The gap, volume and band offsets to the parent compound also exhibit anomalies as function of  $x$ . Specifically, the offsets in epitaxial conditions are predominantly type-B staggered, but have opposite signs in the two end-of-range phases.

## 1. Introduction

The group-III sesquioxides  $\text{Ga}_2\text{O}_3$  and  $\text{In}_2\text{O}_3$  are currently popular in basic materials science and technology for being, respectively, deep-UV large-breakdown and near-UV transparent-conducting materials. A natural development that can be envisaged is the growth of a solid solution  $(\text{Ga}_{1-x}\text{In}_x)_2\text{O}_3$ , typically (but not necessarily) epitaxially on the parent compounds. This would enable one to combine and tune the functionalities of the two parent compounds, and to export the band-engineering and nanostructuration concepts well known in other semiconductor systems (such as arsenides and nitrides) to much higher absorption energies and breakdown voltages.

Progress in this directions requires a knowledge of the miscibility, as well as the behavior of relevant properties (gap, specific volume, band offsets, etc.), of a solid-solution substitutional alloy composed, in a given proportion, of the two parent materials. In this paper we report the modeling of  $(\text{Ga}_{1-x}\text{In}_x)_2\text{O}_3$  over the entire range of  $x$  by (mostly) ab initio density-functional-theory techniques. Previous results [1, 2] for the low- $x$  end of the composition range are integrated in a comprehensive picture of the miscibility and attendant properties. The main result is that the alloy will phase-separate in a large composition range. On the low  $x$  side, the favored phase is isostructural with  $\beta\text{-Ga}_2\text{O}_3$ ; at large  $x$ , it has a bixbyite structure. We also find that as function of  $x$  the gap, volume, and band offsets to the parent compound exhibit discontinuities typical of a first-order phase transition as function of  $x$ .

## 2. Methods and technical issues

Geometry and volume optimizations as well as electronic structure calculations are performed using density-functional theory (DFT) in the generalized gradient approximation (GGA), and the Projector Augmented-Wave (PAW) method as implemented in the VASP code [3].

For mixtures of insulators, it is almost invariably the case that the structure of the mixture is that (or one of those) of the parent compounds. (This certainly does not generally apply to metal alloys.) The stable phase for Ga<sub>2</sub>O<sub>3</sub> is monoclinic  $\beta$ , for In<sub>2</sub>O<sub>3</sub> it is bixbyte. These are discussed at length in previous works ([1] and [4], respectively). While there are no competing structures for In<sub>2</sub>O<sub>3</sub>, for Ga<sub>2</sub>O<sub>3</sub> the  $\beta$  phase can be transformed under pressure into the  $\alpha$  phase; thus we checked these latter phases, and the bixbyte structures. We find that the  $\beta$  phase is lowest in energy; the bixbyte is 80 meV/formula unit higher, and the  $\alpha$  is 250 meV/formula unit higher. We therefore neglect the latter and consider the  $\beta$  and the bixbyte structures.

For the  $\beta$  structure we use, as in [1], supercells containing  $1 \times 2 \times 2$  unit cells (80 atoms) and a  $4 \times 4 \times 2$  k-point grid. For the bixbyte structure, we use the cubic primitive cell (80 atoms), and a  $4 \times 4 \times 4$  k-point grid. The plane wave cutoff is 300 eV, exceeding by 10% or more for all PAW sets the maximum suggested value. The structure of the  $\beta$  phase, reported in [1], is in good agreement with experiment; for bixbyte the lattice constant is 10.29 Å, or 1.5% larger than experiment as usual for GGA calculations.

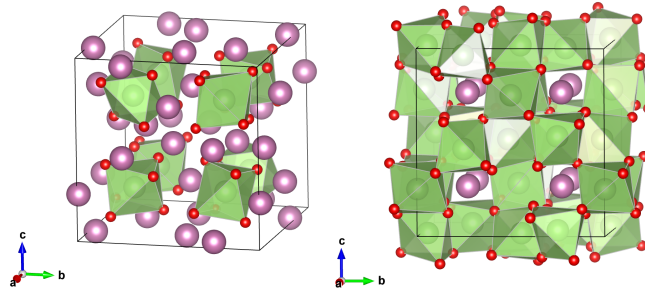


**Figure 1.** The bixbyte structure (group  $T_h$ ) has six-fold coordinated cations (large spheres) occupying  $8b$  high-symmetry and  $24d$  Wyckoff sites. In the left panel we highlight the  $8b$  cation sites by surrounding them with the local octahedra with oxygen (small spheres) at their vertexes; in the right panel we do the same with the  $24d$  lower-symmetry cation sites.

We simulate the compositional variation explicitly mixing In and Ga cations, as dictated by the mole fraction  $x$  of In. For low  $x$ , we consider the monoclinic  $\beta$ -Ga<sub>2</sub>O<sub>3</sub> phase doped with In. This alloy is free-standing, i.e. its energy is calculated at zero stress; we have checked that epitaxial constraints on this phase do not change any of our conclusions, so we neglect them here for clarity. As found previously [2], this phase is only relevant up to about  $x=0.25$ . We then study the bixbyte phase over the whole range of  $x$ ; this is obtained naturally substituting Ga for In in In<sub>2</sub>O<sub>3</sub>, which is indeed a bixbyte as many other sesquioxides [4, 5]. Specifically, we study the bixbyte alloy in two settings: free-standing and In<sub>2</sub>O<sub>3</sub>-epitaxial. In the latter, the in-plane lattice parameters are fixed to that of In<sub>2</sub>O<sub>3</sub> and the vertical lattice parameter and

all internal coordinates are optimized.

Both the  $\beta$  and bixbyite supercells contains 80 atoms, i.e. 32 cations. The choice of configurations in the  $\beta$  phase has been discussed in Ref.[1]. For the bixbyite phase, we find that Ga substitution is slightly favored at the high-symmetry cation site (see Fig.1). We substitute Ga for In on those sites first, and then on the lower symmetry ones. For each  $x$ , we sample a few configurations; as Ga's generally try avoid each other, the geometric constraints on the configurations are stringent, so there are not many possible inequivalent configurations to begin with. Our discussion is based on the lowest energy found at each  $x$ ; of course, these may well not be the absolute energy minima for that  $x$ . Also, we neglect the possible occurrence of higher-energy configurations in small proportions at finite temperature.

### 3. Phase separation

To address the occurrence of phase separation, we calculate the specific (i.e. referred to one cation) Helmholtz free energy (the enthalpy vanishes because the pressure is always zero to numerical accuracy) of the mixture as a function of  $x$ . The internal energy is calculated directly from first principles using the supercells described above. The entropy is modeled as the sum of mixing and vibrational terms. The mixing entropy has the standard form

$$S_m(x) = -x \log x - (1-x) \log (1-x). \quad (1)$$

Since growth temperatures are comparable to or higher than Debye temperatures ( $\Theta_{\text{In}_2\text{O}_3}=420$  K,  $\Theta_{\text{Ga}_2\text{O}_3}=870$  K), the vibrational entropy per cation can be approximated as that of a single-frequency oscillator at the Debye frequency. Thus

$$S_v(x) = 3 [(1+n) \log (1+n) - n \log n], \quad (2)$$

where  $n$  is the Planck-Bose distribution

$$n(T, x) = 1/(e^{\Theta_m(x)/T} - 1), \quad (3)$$

and the mixture's Debye temperature  $\Theta_m(x)$  is assumed to be an interpolation

$$\Theta_m(x) = (1-x) \Theta_{\text{Ga}_2\text{O}_3} + x \Theta_{\text{In}_2\text{O}_3} \quad (4)$$

of that of the parent compounds.

We now recall that phase separation in a mixture occurs when the specific free energy is a negative-curvature function of an extensive parameter such as  $x$ . The values, say,  $x_1 < x_2$ , at which the curvature becomes negative and goes back to positive, respectively, delimit the phase separation region; in general these bounds depend on temperature  $T$ , and the  $x$  range they identify is the miscibility gap. If the negative curvature region vanishes as  $T$  increases, i.e.  $x_1$  and  $x_2$  get to coincide, there is complete miscibility. Our results, as mentioned earlier and discussed below, suggest a large miscibility gap surviving up to above the melting temperatures of the parent compounds. We discuss our results in terms of the *mixing* specific free energy, i.e we subtract out the bulk free energy

$$F_{\text{bulk}}(x) = x F_{\text{In}_2\text{O}_3} + (1-x) F_{\text{Ga}_2\text{O}_3}, \quad (5)$$

which interpolates the values for two equilibrium bulk phases (bixbyite and  $\beta$ , respectively).

Fig.2, left panel, compares the mixing free energies of the free-standing  $\beta$  phase (circles) with that of the epitaxial bixbyite phase (squares). Fig.2, right

panel, compares the same quantities for the same  $\beta$  phase (circles) with that of the free-standing bixbyite phase (diamonds). The temperatures considered are 800 K, a typical growth temperature, and 2000 K, near the melting temperature of the parent compounds. The free energy is evidently upward-convex in a wide region of intermediate  $x$ , indicating that a phase separation occurs. The borders of that region define the miscibility gap.

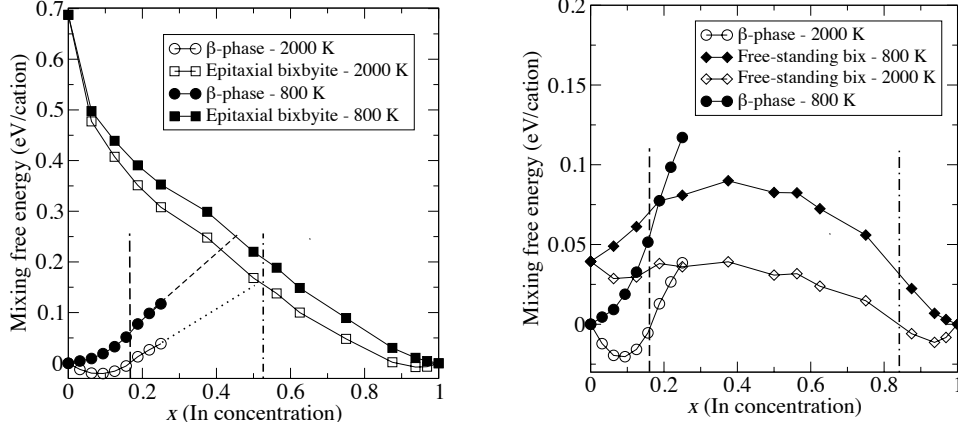


**Figure 2.** Mixing free energy vs  $x$  at 810 K and 2000 K for  $\beta$ -phase vs epitaxial bixbyite (left panel), and  $\beta$ -phase vs free-standing bixbyite (right panel). The phase separation region extends between the vertical dashed and dash-dotted lines.

On the low- $x$  end, the  $\beta$  phase prevails in all cases, and the change in curvature occurs (hence the phase separation region starts) at about  $x \simeq 0.15$ . This confirms largely our previous estimate [1] of 10% maximum In solubility, and experiments [6] giving similar results. At high  $x$ , the end of the miscibility gap region is estimated at  $x \simeq 0.45 \div 0.55$  for the epitaxial case (left panel), subject to large uncertainties in locating the free-energy downturn from the epitaxial phase. Therefore the miscibility gap is approximately  $x \in (0.15, 0.55)$  for the epitaxial bixbyite and  $\beta$  phase. Comparison with the growth and x-ray diffraction study by Zhang *et al.* [7] suggest that this prediction is quite plausible, even accounting for their epitaxial conditions being different from those simulated.

Most importantly, at 2000 K the borders of the phase separation region are about the same as at 800 K, i.e. the miscibility gap hardly changes (it actually may widen slightly). Since the melting temperatures of the parent compounds are around 2200 K, we conclude that in the practical range of  $T$  the miscibility gap between the epitaxial and  $\beta$  phases is  $x \in (0.15, 0.55)$  independent of  $T$ .

We now come to the  $\beta$  phase vs free-standing bixbyite competition (Fig.2, right panel). A phase separation region exists here too, involving the structure change to the  $\beta$  phase at low  $x$ : the lower limit is again  $x = 0.15$ . The free-standing bixbyite phase is favored over the  $\beta$  phase (as well as over the epitaxial) over the rest of the  $x$  range, from  $x = 0.2$  or so onward. However, its own free energy is upward-convex for most of the range; this indicates a phase separation between Ga<sub>2</sub>O<sub>3</sub> and In<sub>2</sub>O<sub>3</sub> *within* the bixbyite phase; the change in curvature on the high  $x$  side is approximately at  $x = 0.8 \div 0.85$ . Therefore the overall miscibility gap is  $x \in (0.15, 0.85)$  in the free-standing case. This is quite clearly the case at both 800 K and 2000 K. Thus, as in the epitaxial

case, we conclude that in the practical range of  $T$  the miscibility gap for free-standing bixbyite is  $x \in (0.15, 0.85)$  independently of  $T$ . An experimental determination of the  $\text{Ga}_2\text{O}_3$ - $\text{In}_2\text{O}_3$  phase diagram [8] suggests that indeed at the In end of the range the single-crystal stability region is quite marginal, being limited to  $x > 0.9$  or so.

#### 4. Gap and volume

Not unexpectedly, the properties of the alloy exhibit anomalies as function of concentration due to the changes in phase and structure. In Fig.3, left panel, we show the calculated optimized volume in the two free-standing bixbyite and  $\beta$  phases, showing a clear volume discontinuity at any given  $x$ . The fundamental gap, shown in Fig.3, right panel, also exhibits analogous interesting features. The  $\beta$  phase has a linear decrease in good agreement with pressure experiments [2, 7]. The bixbyite gap is also linear at low  $x$ , but picks up a significant bowing near  $x=1$ . To correct for the semilocal density-functional error, we supplement the GGA calculated gap with an ad hoc “scissor”-like correction

$$\delta E_g(x) = 2.5x + 2.7(1-x) \text{ eV}, \quad (6)$$

which brings the GGA gap to the experimental value in  $\text{Ga}_2\text{O}_3$  and  $\text{In}_2\text{O}_3$  [9, 10] (incidentally, the correction reduces the bowing as obtained from GGA eigenvalues). Since the lowest gap is dipole-forbidden, to compare with the experimental optical onsets [7] we estimate the position of the optical onset at all  $x$  as the GGA gap value (corrected by Eq.6) plus the difference of optical onset and minimum gap in  $\text{In}_2\text{O}_3$  (0.55 eV).

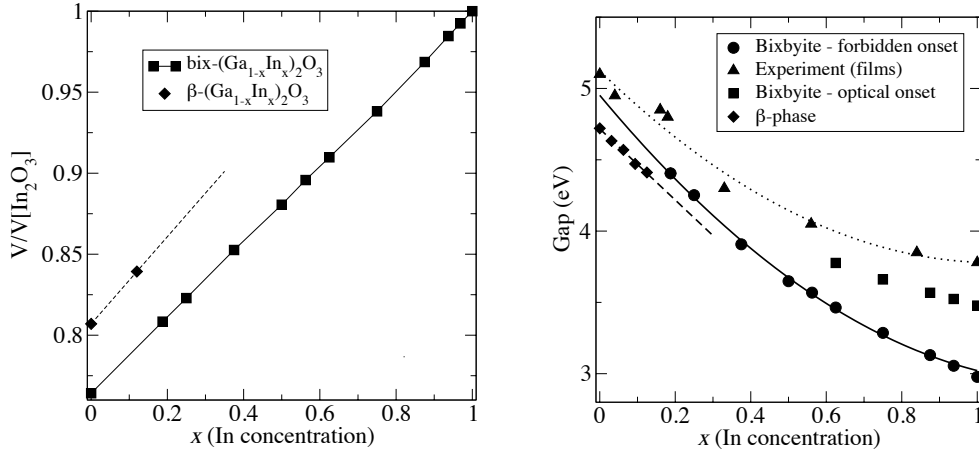


**Figure 3.** Left panel: volume vs mole fraction for the free-standing  $\beta$  and bixbyite phases. Right panel: fundamental gap in the same phases and interpolations vs  $x$  (quadratic for bixbyite; linear at low  $x$  for  $\beta$ ). A correction for the gap error has been introduced (see text). The gap shows a sizable bowing in bixbyite at large  $x$ .

The agreement is decent, but should be taken with more than a grain of salt: on the experiment side, the data are for films grown on sapphire, the In content is generally lower than the nominal one especially at intermediate  $x$ , and the gap in the  $x=0$  and  $x=1$  limits is larger than in most reports (including our own [9]); on

the theory side, we have applied a simple correction that offers no guarantee of being equally appropriate for all transitions and all  $x$ . As we now discuss, an interesting crossover behavior is more easily observable in the band offsets at the interface with the parent compounds.

## 5. Band offsets across the phase transition

Band offsets at interfaces are key quantities in the design and engineering of heterostructures. Ab initio theory has been predicting reliable offsets all along; a review of the theory concepts and of the techniques in common use is in Ref.[11]. Recently we predicted a staggered B-type offset at the (100) interface of  $\beta$ -phase  $\text{Ga}_2\text{O}_3$  with low- $x$   $(\text{Ga}_{1-x}\text{In}_x)_2\text{O}_3$ . Here we extend the work to a much larger range in the bixbyite structure. We simulate the (001)-like interface with  $\text{In}_2\text{O}_3/(\text{Ga}_{1-x}\text{In}_x)_2\text{O}_3$  superlattices epitaxially constrained to  $\text{In}_2\text{O}_3$ , containing 160 atoms in the primitive cell, and with explicit atomic substitutions. We also calculate the same quantities relaxing all lattice parameters of the superlattice; this mimics a substrate that is locally compliant, i.e. deforms along with the film. For  $x$  inside a phase separation region, the calculated values refer to the mixed phase, and not to the potentially compositionally (or structurally) segregated one (see Sec.3).

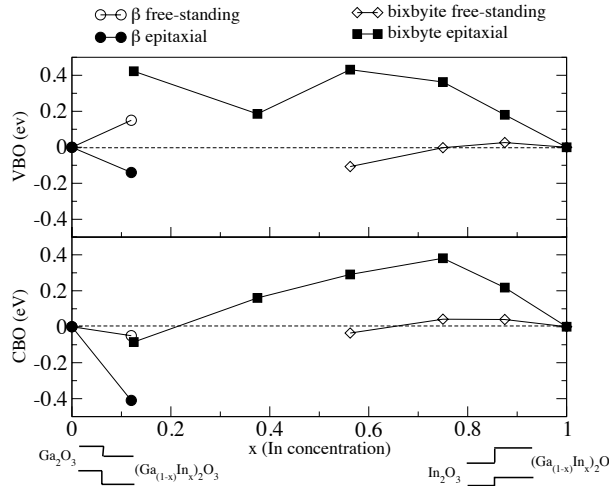


**Figure 4.** Valence (VBO, top) and conduction (CBO, bottom) interface band offsets between  $\text{In}_2\text{O}_3$  and  $(\text{Ga}_{1-x}\text{In}_x)_2\text{O}_3$  in the bixbyite phase, both epitaxially constrained on  $\text{In}_2\text{O}_3$ , or with compliant substrate. The offset between  $\text{Ga}_2\text{O}_3$  and low- $x$   $(\text{Ga}_{1-x}\text{In}_x)_2\text{O}_3$  at  $x \approx 0.1$  in the  $\beta$  phase for the same conditions are also reported.

On the bixbyite side of the phase separation region, the offsets are again type-B (a relatively uncommon occurrence in itself), but most interestingly they are staggered in the opposite direction, i.e. both the conduction and valence offsets encountered in going from the parent compound into the alloy are generally positive, whereas they were negative in the low- $x$  limit (see the sketches in Fig.4). This suggests interesting perspectives for interface offset tuning in this alloy system. The offset values are also rather large, and hence interesting in terms of potential charge confinement. Recalling

the phase separation region discussed above, the most promising  $x$  is around 0.7 in the epitaxial bixbyite. We note that the gap error of density functional theory is immaterial here, as any gap corrections will largely cancel out of the offsets themselves. We thus purposely refer to offsets only, starting from zero at  $x=0$  and  $x=1$ .

## 6. Conclusions

Using (mostly) density-functional ab initio theoretical techniques, we have established that  $(\text{Ga}_{1-x}\text{In}_x)_2\text{O}_3$  will exist in the  $\beta$  phase at low  $x$  and in the bixbyite phase at high  $x$ . For the epitaxial bixbyite case, the compound will phase-separate above 15%, and the two phases will coexist up to about 55%. While the free-standing bixbyite's coexistence with the  $\beta$  phase is limited to about  $x=0.25$ , but bixbyite will itself separate into Ga-rich and In-rich regions for  $x$  up to about 0.85. Thus the effective miscibility gap extends all the way from  $x=0.15$  to  $x=0.85$ . Importantly, both miscibility gaps are practically independent of temperature, and survive up to the melting temperature. The behavior of the calculated volume, gap (in decent agreement with experiments for films), and band offsets also confirm the picture. Interestingly, we find that the interface band offsets are largely type-B staggered and positive at large  $x$ , whereas they are staggered and negative in the low- $x$  limit.

## Acknowledgments

Work supported in part by MIUR-PRIN 2010 project *Oxide*, CAR of University of Cagliari, Fondazione Banco di Sardegna grants, CINECA computing grants. MBM acknowledges the financial support of her PhD scholarship by Sardinia Regional Government under P.O.R. Sardegna F.S.E. Operational Programme of the Autonomous Region of Sardinia, European Social Fund 2007-2013 - Axis IV Human Resources, Objective 1.3, Line of Activity 1.3.1.

## References

- [1] Maccioni M B, Ricci F, and Fiorentini V 2015 *Appl. Phys. Express* **8** 021102.
- [2] Maccioni M B, Ricci F, and Fiorentini V 2014 *J. Phys. Conf. Ser.* **566** 012016.
- [3] Kresse G and Furthmüller J 1996 *Phys. Rev. B* **54** 11169.
- [4] Marsella L and Fiorentini V 2004 *Phys. Rev. B* **69** 172103.
- [5] Delugas P, Fiorentini V, and Filippetti A 2009 *Phys. Rev. B* **80** 104301.
- [6] Baldini M, Gogova D, Irmscher K, Schmidbauer M, Wagner G, and Fornari R 2014 *Cryst. Res. Technol.* **49**, 552.
- [7] Zhang F, Saito K, Tanaka T, Nishio M, Guo Q 2014 *Solid State Comm.* **186** 28.
- [8] Edwards D D, Mason T O, Goutenoire F and Poeppelmeier K R 1997 *Appl. Phys. Lett.* **70** 1706.
- [9] Ricci F, Boschi F, Baraldi A, Filippetti A, Higashiwaki M, Kuramata A, Fiorentini V, and Fornari R 2015, submitted for publication.
- [10] King P D C, Veal T D, Fuchs F, Wang C Y, Payne D J, Bourlange A, Zhang H, Bell G R, Cimalla V, Ambacher O, Egdell R G, Bechstedt F, and McConville C F, 2009 *Phys. Rev. B* **79** 205211.
- [11] Peressi M, Binggeli N, and Baldereschi A, 1998 *J. Phys. D: Appl. Phys.* **31** 1273.